QUANTIZATION AND COMPENSATION IN SAMPLED INTERLEAVED MULTI-CHANNEL SYSTEMS

Shay Maymon, Alan V. Oppenheim

Massachusetts Institute of Technology
Digital Signal Processing Group
77 Massachusetts Avenue, Cambridge MA 02139
maymon@mit.edu, avo@mit.edu

ABSTRACT

This paper considers the environment of interleaved, multi-channel measurements as arises for example in time-interleaved A/D converters and in distributed sensor networks. Such systems take the form of either uniform or recurrent nonuniform sampling, depending on the timing offset between the channels. Quantization in each channel results in an effective overall signal to noise ratio in the reconstructed output which is dependent on the quantizer step sizes, the timing offsets between the channels and the oversampling ratio. Appropriate choice of these parameters together with the design of appropriate compensation filtering is discussed.

Index Terms— Multi-channel sampling, Recurrent nonuniform sampling, Oversampling, Quantization, Interleaved samples

1. INTRODUCTION

In A/D conversion, oversampling is a well established approach to mitigating the effects of quantization, effectively trading off between the oversampling ratio and the required quantization step size for a fixed signal to quantization noise ratio (SQNR). This tradeoff can be accomplished in a direct way by following the quantizer with a low-pass filter and downsampler or by using noise-shaping techniques ([1],[2]). With high bandwidth signals or when large oversampling ratios are desired, time-interleaved A/D converters, using different clock phases are often utilized [3]. With the clock phases appropriately synchronized, the interleaving is equivalent to uniform sampling. Otherwise, the interleaved samples correspond to recurrent nonuniform sampling ([4],[5],[6],[7]). Similarly in a sensor network environment, separate sensors might independently sample a shifted version of an underlying signal with the sensor outputs then transmitted to a fusion center for interleaving and processing.

In this paper we consider the effects of linear quantization in the environment of interleaved, oversampled multi-channel measurements and the design of the optimal filters for each channel prior to combining the results. It is shown for the multi-channel case that with equal quantizer step size in each channel, the resulting overall SQNR is maximized when the channels are exactly synchronized and the system is equivalent to interleaved uniform samples. For the case where the channels are not synchronized, resulting in recurrent nonuniform samples, the SQNR is reduced relative to the uniform case. However, when the quantizer step size is not constrained to be the same in each channel, higher overall SQNR can be achieved by appropriate choice of the compensation filtering and the timing offset between the channels. The concept of having different levels of accuracies in different channels is similar to the approach in sub-band coding ([8],[9]) which provides a way to control and reduce the quantization noise in coding and where each sub-band is quantized with an accuracy based upon appropriate criteria.

This work was supported in part by a Fulbright Fellowship, Texas Instruments Leadership University Program, BAE Systems PO 112991, and Lincoln Laboratory PO 3077828.

2. MULTI-CHANNEL INTERLEAVED SAMPLING AND RECONSTRUCTION

In [6] Papoulis has shown that under some conditions on the multi-channel systems, a bandlimited signal can be perfectly reconstructed from samples of the responses of M linear time-invariant (LTI) systems with the bandlimited signal as their inputs, sampled at $1/M$ times the Nyquist rate. The basic multi-channel sampling and quantization structure considered in this paper is shown in Figure 1. Figure 2 represents the basic structure considered for obtaining uniform samples at the Nyquist rate from the undersampled and quantized multi-channel signals of Figure 1. In the system of Figure 1 the Nyquist rate of the bandlimited signal $x(t)$ is $1/T_N$ and each of the M channels is sampled at a rate of $1/T = 1/(LT_N)$ corresponding to an effective oversampling factor of $\rho = M/L > 1$.

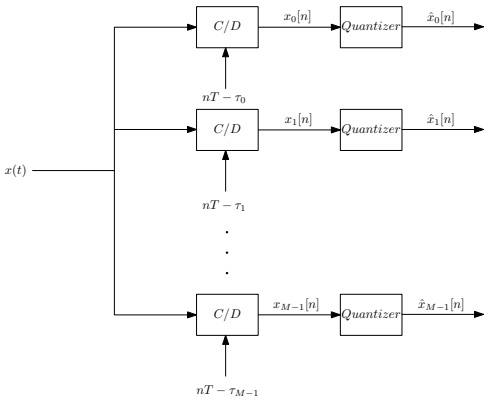

Fig. 1. Multi-channel sampling and quantization

By appropriate choice of the timing offsets τ_m, the outputs can be interleaved to obtain uniformly spaced samples. In the system of Figure 2, the multi-channel outputs of Figure 1 are combined to form uniform samples of $x(t)$ at the Nyquist rate. The filters $G_m(e^{j\omega})$ are chosen to compensate for nonuniform spacing of the channel offsets τ_m and for the quantization noise.

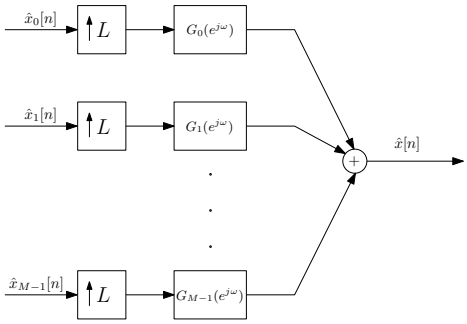

Fig. 2. Multi-channel reconstruction of uniform samples by upsampling followed with filtering

In the absence of error due to quantization, it is straightforward to show that $\hat{x}[n]$ corresponds to uniform samples of $x(t)$ at the Nyquist rate when

$$\sum_{m=0}^{M-1} G_m(e^{j\omega}) \cdot \left[\frac{1}{T} \sum_{k=-(L-1)}^{L-1} X\left(\frac{\omega - \frac{2\pi}{L}k}{T_N} \right) \cdot e^{-j\left(\omega - \frac{2\pi}{L}k\right)\frac{\tau_m}{T_N}} \right]$$
$$= \frac{1}{T_N} X\left(\frac{\omega}{T_N}\right) \quad |\omega| < \pi. \tag{1}$$

Since the sampling rate in each channel is $1/L$ times the Nyquist rate of the input signal, only L shifted replicas of the spectrum of $x(t)$ contribute to each frequency ω in the spectrum of each channel signal $x_m[n]$ in Figure 1. Consequently, at each frequency ω equation (1) imposes L constraints on the M reconstruction filters $G_m(e^{j\omega})$. $L-1$ of these constraints are to remove the aliasing components and one is to preserve $X(\Omega)$. With $M > L$, i.e. with oversampling, there remain $M-L$ degrees of freedom for design of the reconstruction filters to minimize the output average noise power due to quantization.

In our analysis we represent the effect of the linear quantizer in each channel of Figure 1 through an additive noise model ([10, 11, 12]). Specifically, the quantizer output $\hat{x}_m[n]$ in the m^{th} channel is represented as

$$\hat{x}_m[n] = x_m[n] + q_m[n] \tag{2}$$

where $q_m[n]$ is assumed to be an i.i.d random process uniformly distributed between $\pm\Delta_m/2$ and uncorrelated with $x_m[n]$ where Δ_m denotes the quantizer step size. Correspondingly, the variance of $q_m[n]$ is $\sigma_m^2 = {\Delta_m}^2/12$.

To analyze the effect of each channel of Figure 2 on the corresponding quantization noise we consider the system of Figure 3.

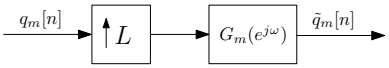

Fig. 3. Single channel in the reconstruction system of Figure 2

The output $\tilde{q}_m[n]$ of the system of Figure 3 is

$$\tilde{q}_m[n] = \sum_{k=-\infty}^{\infty} q_m[k] g_m[n - kL] \tag{3}$$

with $g_m[n]$ as the impulse response corresponds to the frequency response $G_m\left(e^{j\omega}\right)$.

Under the assumption that $q_m[n]$ is a zero-mean i.i.d random process with variance σ_m^2, the autocorrelation function of $\tilde{q}_m[n]$ is

$$R_{\tilde{q}_m\tilde{q}_m}[n, n-l] = \sigma_m^2 \cdot \sum_{k=-\infty}^{\infty} g_m[n - kL] g_m[n - l - kL] \tag{4}$$

which is periodic in n with period L and therefore $\tilde{q}_m[n]$ is a wide-sense cyclostationary random process. Alternatively, $R_{\tilde{q}_m\tilde{q}_m}[n, n-l]$ can be expressed as

$$R_{\tilde{q}_m\tilde{q}_m}[n, n-l] = \frac{1}{2\pi} \int_{-\pi}^{\pi} S_{\tilde{q}_m\tilde{q}_m}(e^{j\omega}; n) \cdot e^{j\omega l} d\omega =$$
$$\frac{1}{2\pi} \int_{-\pi}^{\pi} \left(\sigma_m^2 \cdot {G_m}^*(e^{j\omega}) \cdot E_m^{(n)}(e^{j\omega L}) \cdot e^{-j\omega n} \right) \cdot e^{j\omega l} d\omega \tag{5}$$

where $E_m^{(n)}(e^{j\omega})$ are the discrete-time Fourier transforms of the polyphase components $e_m^{(n)}[k]$ of $g_m[n]$ defined as

$$e_m^{(n)}[k] = g_m[n + kL] \quad n = 0, 1, \ldots, L-1, \quad k = 0, \pm 1, \ldots \tag{6}$$

and for which

$$G_m(e^{j\omega}) = \sum_{n=0}^{L-1} E_m^{(n)}(e^{j\omega L}) \cdot e^{-j\omega n}. \tag{7}$$

The polyphase representation of $G_m(e^{j\omega})$ in (7) suggests an alternative implementation of the reconstruction system of Figure 2. If finite impulse response (FIR) filters are used for the impulse responses $g_m[n]$ of the reconstruction filters, considerable gain in computational efficiency can be achieved by utilizing the polyphase decomposition of $G_m(e^{j\omega})$ and rearranging the operations so that the filtering is done at the low sampling rate.

From (4), the ensemble average power $E(\tilde{q}_m^2[n])$ of $\tilde{q}_m[n]$ is periodic with period L. Averaging also over time and denoting by $\sigma_{\tilde{q}_m}^2$ the time and ensemble average power of $\tilde{q}_m[n]$ we obtain

$$\sigma_{\tilde{q}_m}^2 = \frac{1}{L} \sum_{n=0}^{L-1} E(\tilde{q}_m^2[n]) = \frac{1}{L} \sum_{n=0}^{L-1} R_{\tilde{q}_m\tilde{q}_m}[n, n]. \tag{8}$$

Expressing $R_{\tilde{q}_m\tilde{q}_m}[n, n]$ in terms of $S_{\tilde{q}_m\tilde{q}_m}(e^{j\omega}; n]$ as in (5) and using eq. (7), eq. (8) becomes

$$\sigma_{\tilde{q}_m}^2 = \frac{\sigma_m^2}{2\pi L} \cdot \int_{-\pi}^{\pi} {G_m}^*(e^{j\omega}) \cdot \left(\sum_{n=0}^{L-1} E_m^{(n)}(e^{j\omega L}) \cdot e^{-j\omega n} \right) d\omega$$
$$= (\sigma_m^2/L) \cdot \frac{1}{2\pi} \int_{-\pi}^{\pi} |G_m(e^{j\omega})|^2 d\omega. \tag{9}$$

We denote by $e[n]$ the total noise component in $\hat{x}[n]$ due to quantization in the system of Figure 2, i.e.

$$e[n] = \sum_{m=0}^{M-1} \tilde{q}_m[n] \tag{10}$$

where as defined in Figure 3, $\tilde{q}_m[n]$ is the quantization noise output in the m^{th} channel of the reconstruction system. Then, based on (9) and with the assumption that the quantization noise is uncorrelated between channels, the time and ensemble average power of $e[n]$ denoted by σ_e^2, is

$$\sigma_e^2 = \frac{1}{L} \sum_{n=0}^{L-1} E\left(e^2[n]\right) = \sum_{m=0}^{M-1} \left(\frac{1}{L} \sum_{n=0}^{L-1} E(\tilde{q}_m^2[n]) \right) =$$
$$\sum_{m=0}^{M-1} \sigma_m^2/L \cdot \frac{1}{2\pi} \int_{-\pi}^{\pi} |G_m(e^{j\omega})|^2 \, d\omega. \tag{11}$$

We choose the optimal reconstruction filters $G_m(e^{j\omega})$ to minimize σ_e^2 under the following set of constraints

$$\sum_{m=0}^{M-1} G_m(e^{j\omega}) \cdot e^{-j(\omega-\frac{2\pi}{L}k)\tau_m/T_N} = L \cdot \delta[k] \quad \omega \in \Delta\omega_i,$$
$$k = -i, -i+1, \ldots, L-1-i, \quad i = 0, 1, \ldots, L-1 \tag{12}$$

which follows directly from equation (1) and where $\Delta\omega_i = \left[\pi - (i+1)\frac{2\pi}{L}, \pi - i\frac{2\pi}{L}\right]$. This optimization results in

$$G_m(e^{j\omega}) = 1/\sigma_m^2 \cdot \left(\sum_{l=-i}^{L-1-i} \lambda_l^{(i)} \cdot e^{-j2\pi(\tau_m/LT_N)l}\right) \cdot e^{j\omega\tau_m/T_N}$$
$$\omega \in \Delta\omega_i, \quad i = 0, 1, \ldots, L-1, \quad m = 0, 1, \ldots, M-1 \tag{13}$$

where for each $i = 0, 1, \ldots, L-1$ the sequence $\{\lambda_k^{(i)}\}_{k=-i}^{L-1-i}$ is defined as the solution to the following set of equations

$$\sum_{k=0}^{L-1} A_{lk} \cdot \lambda_{k-i}^{(i)} = L \cdot \delta[l-i] \quad l = 0, 1, \ldots, L-1 \tag{14}$$

with A an LxL Hermitian Toeplitz matrix such that

$$A = \sum_{m=0}^{M-1} (\underline{v}_m \cdot \underline{v}_m{}^H)/\sigma_m^2 \tag{15}$$

and

$$\underline{v}_m{}^H = \left[1, e^{-j2\pi\frac{\tau_m}{LT_N}}, \ldots, e^{-j2\pi\frac{\tau_m}{LT_N}(L-1)}\right]. \tag{16}$$

An alternative representation of the optimal choice of $G_m(e^{j\omega})$ is

$$G_m(e^{j\omega}) = 1/\sigma_m^2 \cdot \Lambda^{(i)}(e^{j\omega_m}) \cdot e^{j\omega\tau_m/T_N} \quad \omega \in \Delta\omega_i$$
$$i = 0, 1, \ldots, L-1, \quad m = 0, 1, \ldots, M-1 \tag{17}$$

where $\Lambda^{(i)}(e^{j\omega_m})$ is the discrete-time Fourier transform of the finite-length sequence $\{\lambda_k^{(i)}\}_{k=-i}^{L-1-i}$ frequency sampled at

$$\omega_m = 2\pi\tau_m/(LT_N). \tag{18}$$

Substituting the expression for $G_m(e^{j\omega})$ from (17) into (11) we obtain for the minimum achievable value of σ_e^2

$$\sigma_{emin}^2 = \frac{1}{L}\sum_{i=0}^{L-1}\left(\frac{1}{L}\sum_{m=0}^{M-1}|\Lambda^{(i)}(e^{j\omega_m})|^2/\sigma_m^2\right) \tag{19}$$

which can be also shown to be equal to $tr(A^{-1})$. Noting that the equation corresponds to $l = i$ in (14) is

$$\sum_{m=0}^{M-1} 1/\sigma_m^2 \cdot \Lambda^{(i)}(e^{j\omega_m}) = L, \tag{20}$$

and applying the Cauchy-Schwartz inequality to it results in

$$\sum_{m=0}^{M-1} 1/\sigma_m^2 \cdot \sum_{m=0}^{M-1} |\Lambda^{(i)}(e^{j\omega_m})|^2/\sigma_m^2 \geq L^2 \tag{21}$$

for each $i = 0, 1, \ldots, L-1$. Therefore, together with eq. (19) it follows that

$$\sigma_{emin}^2 \geq \frac{L}{\sum_{m=0}^{M-1} 1/\sigma_m^2} \tag{22}$$

where equality is achieved if and only if any of the following equivalent conditions is satisfied

$$\Lambda^{(i)}(e^{j\omega_m}) = \frac{L}{\sum_{n=0}^{M-1} 1/\sigma_n^2} \qquad \begin{matrix} i = 0, 1, \ldots, L-1 \\ m = 0, 1, , \ldots, M-1 \end{matrix} \tag{23a}$$

$$\sum_{m=0}^{M-1} 1/\sigma_m^2 \cdot e^{j\omega_m l} = 0 \quad l = 1, 2, \ldots, L-1 \tag{23b}$$

$$\lambda_k^{(i)} = \frac{L}{\sum_{m=0}^{M-1} 1/\sigma_m^2}\delta[k] \quad k = -i, -i+1, \ldots, L-1-i. \tag{23c}$$

3. UNIFORM AND RECURRENT NONUNIFORM INTERLEAVED SAMPLING - QUANTIZATION NOISE ANALYSIS

For the system of Figure 2 with the quantization step size the same in each channel, we next show that equations (22) and (23) imply that σ_{emin}^2 is minimized, i.e. equality is achieved in (22) when the interleaved multi-channel system corresponds to uniform sampling. In this case

$$\sigma_{emin}^2 = (L/M) \cdot \sigma^2 \tag{24}$$

where σ^2 denotes the variance of the quantization noise source in each channel. To show this we note that with $\sigma_m^2 = \sigma^2$, the condition of eq. (23b) becomes

$$\sum_{m=0}^{M-1} e^{j\omega_m l} = 0 \quad l = 1, 2, \ldots, L-1, \tag{25}$$

which is clearly satisfied for any L and M when the values $e^{j\omega_m}$ are uniformly spaced on the unit circle, corresponding to interleaved uniform sampling. However many other distributions of ω_m satisfy eq. (25).

Figure 4 shows the factor $\gamma = \sigma^2/\sigma_{emin}^2$ representing the reduction in the average noise power as a function of the delays τ_1 and τ_2 as a result of the reconstruction of Figure 2 with $M = 3$, $L = 2$ and $\tau_0 = 0$. As indicated, the maximum noise reduction is achieved for $\tau_1 = -\tau_2 = \pm(2/3) \cdot T_N$ for which $\sigma_{emin}^2 = (2/3) \cdot \sigma^2$. This corresponds to interleaving of the channels resulting in uniform sampling and an oversampling of $3/2$.

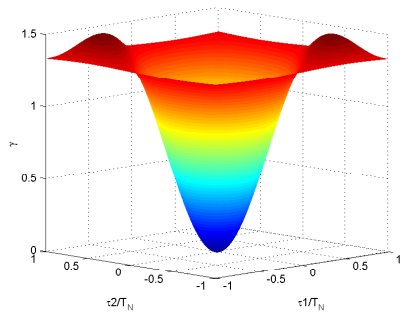

Fig. 4. The reduction factor γ in the average noise power as a function of the delays τ_1 and τ_2 as a result of the reconstruction of Figure 2 with $M = 3$, $L = 2$ and $\tau_0 = 0$

Interestingly, for every other choice of delays for which the sampling corresponds to recurrent nonuniform sampling, the average power of the quantization noise is larger.

In summary, it follows from eq. (22) and illustrated in the preceding example that for the reconstruction structure suggested in Figure 2 and with the quantization step size the same in each channel, the uniform sampling grid achieves the minimum average quantization noise power $(L/M) \cdot \sigma^2$. Any other choice of τ_m which corresponds to a recurrent nonuniform grid and for which (25) is not satisfied results in a higher average quantization noise power.

However, as we next show, by allowing the quantization step size to be chosen separately for each channel, so that quantization noise sources $q_m[n]$ in the different channels have different variances σ_m^2, better SQNR can be achieved. For comparison purposes, we will assume that the average power of the quantization noise sources in all channels is equal to the quantization noise power in each channel in our previous analysis [1] , i.e.

$$\frac{1}{M}\sum_{m=0}^{M-1}\sigma_m^2 = \sigma^2. \tag{26}$$

Applying the Cauchy-Schwartz inequality into the identity $\sum_{m=0}^{M-1}\sigma_m \cdot 1/\sigma_m = M$, it follows that

$$\sum_{m=0}^{M-1}\sigma_m^2 \cdot \sum_{m=0}^{M-1} 1/\sigma_m^2 \geq M^2 \tag{27}$$

and equivalently

$$\frac{L}{\sum_{m=0}^{M-1} 1/\sigma_m^2} \leq (L/M)\cdot\sigma^2 \tag{28}$$

with equality if and only if

$$\sigma_m^2 = \sigma^2 \qquad m = 0, 1, \ldots, M-1. \tag{29}$$

Together with (22), we conclude that by having different levels of accuracies in the quantizers in the different channels, it might be possible to reduce the average quantization noise power. This suggests a way to compensate for the mismatch in the delays in the elements of Figure 1 and increase the total SQNR. Alternatively, we can deliberately introduce delays in the channels so that with appropriate design of the quantizers, we will achieve better SQNR as compared to the equivalent uniform sampling with equal quantizer step size in each channel. The analysis and conclusions of course depend on the validity of the additive noise model used for the quantizer which becomes less appropriate as the quantizer step size increases.

It can be shown by using properties of the Fourier transform that for the case where the quantizer step size is not the same in each channel and the oversampling ratio $1 < \rho < 2$, the minimum average quantization noise power in eq. (22) cannot be achieved with uniform sampling. However, even when the delays correspond to uniform sampling, it might be possible to achieve better SQNR by not constraining the step size to be the same in each channel.

We next demonstrate that with appropriate design of the quantizer in each channel we can compensate for the mismatch in the delays in the elements of Figure 1. As an example, we consider the system of Figure 1 with $M = 3$ and $L = 2$ corresponding to oversampling of $3/2$. When the delay offsets are $\tau_0 = 0$, $\tau_1 = 0.29T_N$ and $\tau_2 = -0.75T_N$ and the quantization step size is the same in each channel (corresponding to $\sigma^2 = 1$), $\sigma_{e^2_{min}} = 0.734$, as indicated in Table 1. As expected, the SQNR is reduced relative to the case where the channel offsets chosen to correspond to interleaved uniform sampling for which $\sigma_{e^2_{min}} = 2/3$. However, when the quantizer step size is not constrained to be the same in each channel, better SQNR can be obtained. Specifically, choosing σ_m^2 to satisfy the condition in (23b) or equivalently to achieve equality in (22) subject to the constraint in (26) results in $\sigma_0^2 = 2.246$, $\sigma_1^2 = 0.398$ and $\sigma_2^2 = 0.356$ which corresponds to $\sigma_{e^2_{min}} = L/(\sum_{m=0}^{M-1} 1/\sigma_m^2) = 0.347$. Note that the large offset between channel 2 and the other two channels is compensated with better accuracy of the quantizer in this channel. Another interesting scenario is that in which different levels of accuracies exist in the different channels of the multi-channel sampling system. Setting the delays such that the interleaving is equivalent to uniform sampling is in general not the optimal choice. Specifically, when $\sigma_0^2 = 2.246$, $\sigma_1^2 = 0.398$ and $\sigma_2^2 = 0.356$, the output average noise power $\sigma_{e^2_{min}}$ obtained for equally spaced delays is 0.408 as compared to 0.347 which is the lower bound on $\sigma_{e^2_{min}}$ achieved by $\tau_0 = 0$, $\tau_1 = 0.29T_N$ and $\tau_2 = -0.75T_N$. The following table summarizes these four cases.

$(\tau_0, \tau_1, \tau_2) \setminus (\sigma_0^2, \sigma_1^2, \sigma_2^2)$	$(1, 1, 1)$	$(2.246, 0.398, 0.356)$
$(0, 2/3T_N, -2/3T_N)$	$\sigma_{e^2_{min}} = 2/3$	$\sigma_{e^2_{min}} = 0.408$
$(0, 0.29T_N, -0.75T_N)$	$\sigma_{e^2_{min}} = 0.734$	$\sigma_{e^2_{min}} = 0.347$

Table 1. The output average noise power

[1] Other constraints on the total number of bits may be considered instead

4. REFERENCES

[1] Alan V. Oppenheim and Ronald W. Schafer, *Discrete-Time Signal Processing*, Prentice Hall, 2010.

[2] J.C. Candy and G.C. Temes, *Oversampling Delta-Sigma Data Converters*, IEEE Press New York, NY, 1992.

[3] W. C. Black Jr. and D. A. Hodges, "Time interleaved converter arrays," *IEEE J. Solid-State Circuits*, vol. SC-15, pp. 1022–1029, Dec 1980.

[4] J. L. Yen, "On nonuniform sampling of bandwidth-limited signals," *IRE Trans. Circ. Theory*, vol. 3, no. 4, pp. 251–257, 1956.

[5] Abdul J. Jerri, "The Shannon sampling theorem-its various extensions and applications: A tutorial review," *Proceedings of the IEEE*, vol. 65, no. 11, pp. 1565–1596, 1977.

[6] A. Papoulis, "Generalized sampling expansion," *IEEE Trans. Circuits and Systems*, vol. CAS-24, no. 11, pp. 652–654, 1977.

[7] Y. C. Eldar and A. V. Oppenheim, "Filterbank reconstruction of bandlimited signals from nonuniform and generalized samples," *IEEE Trans. Signal Processing*, vol. 48, no. 10, pp. 2864–2875, 2000.

[8] R. E. Crochiere, S. A. Webber, and J. L. Flanagan, "Digital coding of speech in sub-bands," *Bell System Technical Journal*, vol. 55, no. 8, pp. 10691085, 1976.

[9] Martin Vetterli and Jelena Kovacevic, *Wavelets and Subband Coding*, Prentice Hall, 1995.

[10] W.R. Bennett, "Spectra of quantized signals," *Bell System Technical J.*, vol. 27, pp. 446–472, 1948.

[11] Anekal B. Sripad and Donald L. Snyder, "A necessary and sufficient condition for quantization errors to be uniform and white," *IEEE Trans. Acoustics, Speech, and Signal Processing*, vol. ASSP-25, no. 5, pp. 442–448, 1977.

[12] Bernard Widrow, Istvan Kollar, and Ming Chang Liu, "Statistical theory of quantization," *IEEE Trans. Instrumentation and Measurement*, vol. 45, no. 2, pp. 353–361, 1996.